The Journal of International Advanced Otology

J Int Adv Otol 2025; 21(5): 1–10 • DOI: 10.5152/iao.2025.251965

Original Article

White Matter Changes in Cases with Unilateral Idiopathic Sudden Sensorineural Hearing Loss Indicated by Diffusion Tensor Imaging Based on Tract-Based Spatial Statistics

Lin Zhang[1], Siying Li[1], Fangfang Chen[1], Yating Wang[2], Mengqi Wang[2], Rui Ma[1]

[1]Department of Radiology, Jining No.1 People's Hospital, Shandong, China
[2]Department of Otolaryngology (ENT), Jining No.1 People's Hospital, Shandong, China

ORCID IDs of the authors: L.Z. 0000-0003-3061-5527; S.L. 0009-0006-9868-435X, F.C. 0009-0005-3061-4286, Y.W. 0009-0008-4057-2958, M.W. 0009-0001-4012-736X, R.M. 0009-0002-0138-1602.

Cite this article as: Zhang L, Li S, Chen F, Wang Y, Wang M, Ma R. White matter changes in cases with unilateral idiopathic sudden sensorineural hearing loss indicated by diffusion tensor imaging based on tract-based spatial statistics. *J Int Adv Otol.* 2025, 21(5), 1965, doi:10.5152/iao.2025.251965.

BACKGROUND: To characterize alterations in white matter microstructure in cases with idiopathic sudden sensorineural hearing loss (SSNHL) through tract-based spatial statistics applied to diffusion tensor imaging (DTI), elucidating both early-stage and chronic neuroanatomical alterations.

METHODS: All cases underwent high-resolution conventional magnetic resonance imaging and DTI. Diffusion data preprocessing was performed using the FMRIB Software Library, including corrections for eddy currents and head motion, brain extraction, and normalization to standard space. Tract-based spatial statistics was employed to undertake voxel-wise whole-brain analysis of fractional anisotropy (FA), mean diffusivity (MD), and radial diffusivity across 3 groups: left-sided idiopathic SSNHL, chronic left-sided sensorineural hearing loss (SNHL), and healthy control (HC). Additionally, in the SNHL group, correlation analysis of regional DTI metrics with clinical variables was implemented, involving disease duration, interaural latency difference, and auditory brainstem response thresholds.

RESULTS: Relative to the HC group, the left SNHL group exhibited remarkably diminished FA values in the bilateral internal capsules, superior corona radiata, and left external capsule. Concurrently, elevated MD values were noteworthy in the body of the corpus callosum, left external capsule, bilateral internal capsules, and corona radiata. Radial diffusivity values were escalated in the corpus callosum body, bilateral superior corona radiata, and left external capsule, suggesting compromised microstructural integrity.

CONCLUSION: Both idiopathic SSNHL and chronic SNHL cases demonstrated discernible white matter abnormalities, implicating a disruption in major commissural and projection fiber tracts. Notably, cases with prolonged auditory deprivation exceeding 2 years exhibited microstructural signatures consistent with axonal degeneration and progressive demyelination.

KEYWORDS: Auditory brainstem response, diffusion tensor imaging, spatial statistical analysis based on fiber bundle tracing, sudden deafness

INTRODUCTION

Sudden sensorineural hearing loss (SSNHL) is clinically characterized by a sudden onset of rapidly progressive auditory dysfunction, operationally defined as a minimum threshold shift of 30 dB affecting at least 3 contiguous audiometric frequencies within a 72-hour window.[1] This condition is frequently regarded as an otologic emergency due to its acute presentation and potential for irreversible auditory impairment. Owing to the largely obscure etiology and pathophysiological mechanisms underlying SSNHL, conventional diagnostic modalities are frequently insufficient in elucidating a definitive causative pathology. Consequently, a substantial proportion of SSNHL cases are designated as idiopathic SSNHL (ISSNHL), reflecting the absence of an identifiable etiology despite comprehensive clinical assessment. A multitude of potential mechanisms, involving vascular insufficiency, viral-induced cochlear inflammation, and aberrant autoimmune responses, have been documented earlier.[2,3] Nonetheless, in the vast majority

Corresponding Author: Rui Ma e-mail: 15668182711@163.com
Received: March 22, 2025 • **Revision Requested:** April 10, 2025 • **Last Revision Received:** April 17, 2025 • **Accepted:** June 26, 2025 • **Publication Date:** September 1, 2025
Available online at www.advancedotology.org

of cases, the precise pathogenic cascade remains indeterminate, thereby impeding the formulation of evidence-based therapeutic strategies.[4]

While high-resolution computed tomography and standard magnetic resonance imaging (MRI) are advantageous for detecting gross structural abnormalities, including congenital malformations of the temporal bone, neoplastic lesions in the internal auditory canal, and cerebrovascular insults, such as acute infarction, these modalities exhibit limited sensitivity in the context of SSNHL lacking anatomical disruptions. In contrast, diffusion tensor imaging (DTI), an advanced non-invasive MRI technique, enables the in vivo quantification of microstructural integrity in white matter (WM) tracts by modeling the anisotropic diffusion of water molecules.[5,6] Analytical methodologies in DTI involve region-of-interest (ROI) assessment, voxel-based morphometry, and quantitative tractography. Empirical investigations utilizing DTI have consistently demonstrated microstructural perturbations in the WM architecture of cases with sensorineural hearing loss, implicating both canonical auditory pathways, including the lateral lemniscus, inferior colliculus, auditory cortex, and auditory radiations, as well as extra-auditory regions.[7–12] These alterations have been interpreted as indicative of axonal degeneration and/or dysmyelination secondary to auditory deprivation. Despite the expanding body of literature delineating WM anomalies in SNHL populations, investigations specifically addressing SSNHL remain relatively underrepresented. To address this gap, the present study employed tract-based spatial statistics (TBSS) to systematically characterize whole-brain WM microstructural alterations in idiopathic SSNHL patients, thereby providing neuroanatomical insights that may be valuable for the development of more individualized and mechanistically grounded therapeutic approaches.

METHODS

Participants

A total of 33 patients experiencing their first episode of left-sided SSNHL, 21 patients with left-sided SNHL lasting more than 2 years, and 35 age- and gender-matched healthy controls were recruited between 2021 and 2023. All participants were right-handed. Written informed consent was obtained from each case prior to their recruitment. Comprehensive clinical and audiometric datasets were precisely compiled for all enrolled subjects, involving demographic variables (age and sex), alongside detailed audiological evaluations. An attemp was made to acquire the study protocol's authorization from the Institutional Review Board of University of Jining No.1 People's Hospital, with the approval number 2024-IIT-082, particularly granted on June 1, 2024.

An attempt was made to stringently define the following inclusion criteria: (1) fulfillment of the established diagnostic criteria for idiopathic SSNHL, with undetectable structural abnormalities in either peripheral or central auditory pathways on routine anatomical MRI; (2) for the SSNHL group, a first-onset episode with a disease course of ≤14 days at the time of neuroimaging; and (3) for the chronic SNHL group, persistent auditory dysfunction extending for a minimum of 2 years subsequent to the initial idiopathic SSNHL diagnosis, confirming long-term sensory deprivation.

An attempt was made to stringently define the following exclusion criteria: (1) MRI contraindications; (2) a history of ear infections, noise-induced trauma, ototoxic drug exposure, or otologic surgery; and (3) the presence of retro-cochlear or neurological conditions, such as tumors, trauma, infections, strokes, or other neural disorders.

Magnetic Resonance Imaging Acquisition

All cases underwent neuroimaging on a Siemens 3.0 Tesla MRI system acquired from Siemens Medical Solutions, headquartered in Erlangen (Germany), equipped with a 16-channel phased-array head coil optimized for high-resolution diffusion imaging. The MRI protocols included the following sequences: (1) T1WI:TE = 9.2 ms, TR = 20 000 ms, FOV = 230 mm × 230 mm, slice thickness = 5 mm; (2) T2WI:TE = 99 ms, TR = 35 000 ms, FOV = 230 mm × 230 mm, slice thickness = 5 mm; (3) T2-FLAIR:TR = 80 000 ms, TE = 83 ms, FOV = 230 mm × 230 mm, slice thickness = 5 mm.

DTI:TE = 91 ms, TR = 10 000 ms, slice thickness = 2 mm, FOV = 256 mm × 256 mm, voxel size = 2 mm × 2 mm × 2 mm, b = 0, 1000 s/mm^2, direction = 30.

Tract-Based Spatial Statistics Analysis

Diffusion tensor imaging dataset processing was performed through the FMRIB Software Library (FSL; www.fmrib.ox.ac.uk/fsl), a comprehensive neuroimaging analysis platform. An attempt was made to

Table 1. Demographic and Clinical Data of All Subjects

	Idiopathic SSNHL Group	SNHL Group	HC Group	χ^2/F	*P*
Number (n)	30	20	35	–	–
Gender (Male/Female)	12/18	9/11	16/19	0.238	.888[a]
Age (Years)	46.30 ± 15.14	43.25 ± 14.46	43.03 ± 11.71	0.537	.586[b]
Course of disease (days/years)*	5.33 ± 3.50	2.43 ± 0.42	–	–	–
ABR threshold (dBnHL)	–	57.5 ± 20.229	–	–	–
ILD (ms)	–	0.46 ± 0.12	–	–	–

Statistical analyses for comparisons between groups were carried out with χ^2 tests[a] or single factor analysis of variance[b].
ABR, auditory brainstem response; HC, health control; ILD, interaural latency difference; SNHL, sensorineural hearing loss; SSNHL, sudden sensorineural hearing loss.
*Time measured in days in idiopathic SSNHL group, and years in SNHL group.

MAIN POINTS

- This study provided new insights into the early and progressive changes in white matter microstructure associated with sudden sensorineural hearing loss and chronic sensorineural hearing loss.
- The findings suggested that hearing loss could lead to structural alterations in commissural, projection, and association fibers, with progressive demyelination over time.
- Sensorineural hearing loss patients with a disease duration exceeding 2 years exhibited axonal damage and demyelination.

preprocess raw diffusion-weighted images to correct for eddy current-induced geometric distortions and subject motion artifacts to a reference volume using FMRIB's Diffusion Toolbox. Brain extraction was subsequently performed employing the Brain Extraction Tool to eliminate non-neural tissue, thereby optimizing downstream registration accuracy. FA maps' generation was conducted, followed by nonlinear spatial normalization to the MNI152 standard template via FMRIB's Nonlinear Image Registration Tool, ensuring inter-subject

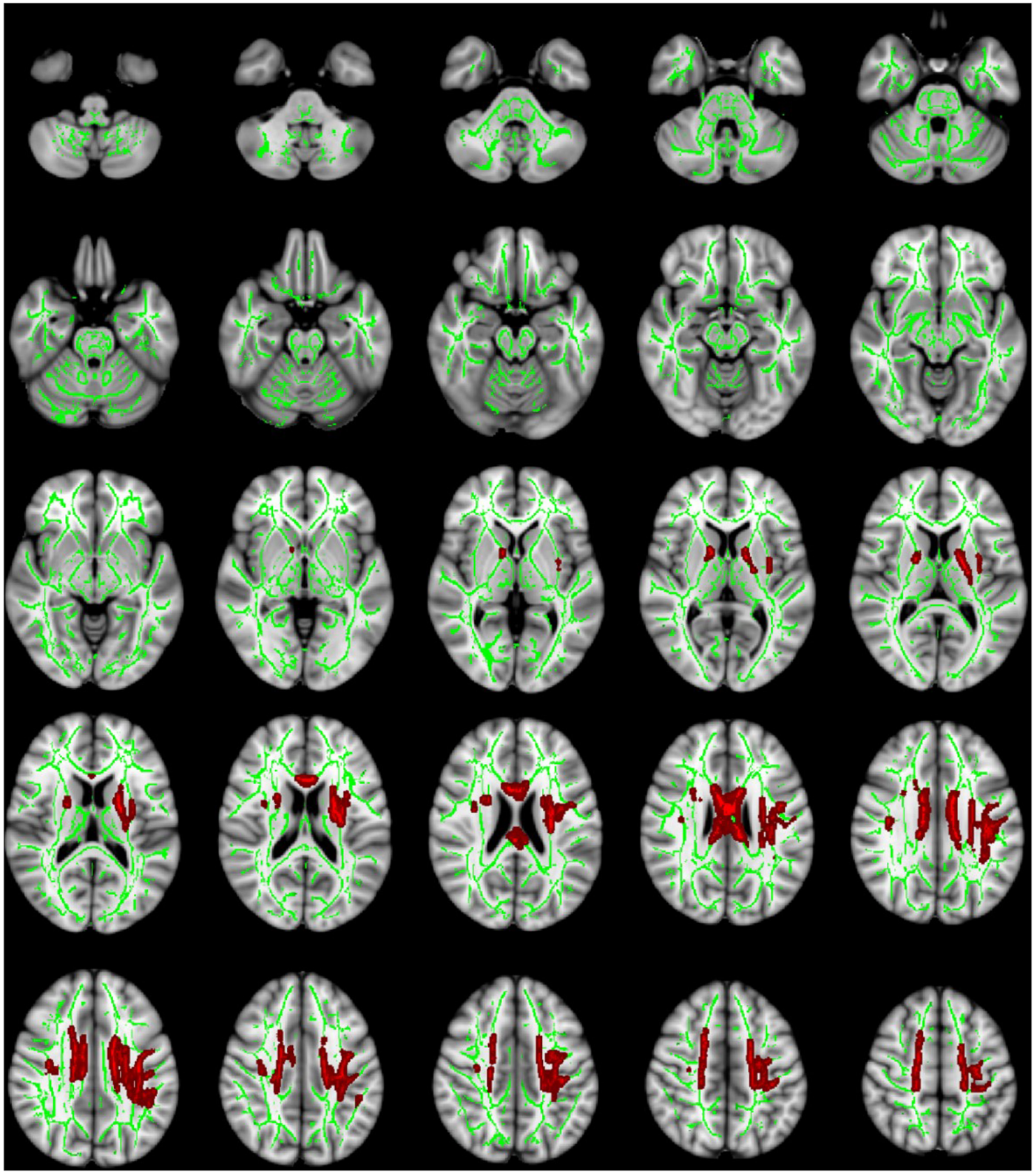

Figure 1. Whole-brain group comparison of mean diffusivity values obtained through tract-based spatial statistics analysis ($P < .05$) between the idiopathic sudden sensorineural hearing loss and healthy control groups.

Table 2. Summary of Diffusion Tensor Imaging Parameters Showing Significant Differences Between the Idiopathic Sudden Sensorineural Hearing Loss Group and the Healthy Control Group

	Cluster Index	Voxel Size in Total	*P*	Peak MNI			Atlases (JHU ICBM-DTI-81)	Ratio of Voxels
				X	Y	Z		
MD	1	7377	.001	92	132	96	Body of corpus callosum	41.2
				118	117	94	Superior corona radiata L	20.5
				123	110	109	Superior longitudinal fasciculus L	16.1
				110	129	86	Anterior limb of internal capsule L	5.6
				120	122	89	External capsule L	5.3
				110	121	83	Posterior limbs of the internal capsules L	4.6
				117	92	98	Posterior corona radiata L	3.4
	2	220	.001	78	128	79	Anterior limb of internal capsule R	45.2
				66	128	94	Superior corona radiata R	24.5
				69	128	96	Superior fronto-occipital fasciculus R	15.6
				70	125	81	Posterior limbs of the internal capsules R	9.45
	3	123	.001	55	116	105	Superior longitudinal fasciculus R	95.3

The mean diffusivity value of the idiopathic sudden sensorineural hearing loss group is higher. Height threshold $P = .05$.
DTI, diffusion tensor imaging; ICBM, international consortium for brain mapping; JHU, Johns Hopkins University; L, left; MD, mean diffusivity; MNI, Montreal neurological institute; R, right.

anatomical correspondence. A mean FA skeleton (representing the core architecture of major WM tracts across subjects) was computed by averaging aligned FA maps and setting a threshold at FA > 0.2 to exclude voxels with insufficient anisotropic signal, thus minimizing the inclusion of peripheral or non-WM voxels. In parallel, secondary diffusion scalar metrics, including mean diffusivity (MD), radial diffusivity (RD), and axial diffusivity (AD), were derived in accordance with previously validated computational frameworks.

Subsequent voxel-wise statistical inference across subjects was performed through the Randomise tool in FSL, implementing a nonparametric permutation testing framework with 5000 iterations to robustly assess intergroup contrasts via two-sample t-tests. To mitigate the inflated type 1 error rate inherent in voxel-wise comparisons, threshold-free cluster enhancement was applied, followed by stringent correction for multiple comparisons using family-wise error control, with statistical significance conservatively set at a corrected threshold of $P < .05$. Only spatially contiguous clusters exceeding a minimum volume of 100 voxels were retained for further interpretation. For neuroanatomical localization, statistically significant clusters were co-registered to the Johns Hopkins University International Consortium for Brain Mapping ICBM-DTI-81 WM atlas, facilitating accurate regional annotation in standard Montreal Neurological Institute (MNI) space. Diffusion metric values were subsequently extracted from these clusters to enable detailed quantitative assessments.

Statistical Analysis

Statistical analysis's implementation was through SPSS 26.0 software (IBM SPSS Corp.; Armonk, NY, USA). Intergroup differences, particularly in categorical variables, involving age distribution, were evaluated via the chi-squared test. The distributional characteristics of continuous variables were examined using the Shapiro–Wilk test to assess assumptions of normality. For continuous variables conforming to parametric assumptions, the utilization of one-way ANOVA was noteworthy to compare group-level differences. To elucidate the link of regional microstructural alterations with clinical phenotypes, particularly in the left-sided SSNHL group, it was attempted to implement Pearson correlation analysis between DTI-derived metrics from significant clusters and clinical parameters, involving disease duration, interaural level difference (ILD), and auditory brainstem response (ABR) thresholds. Indication of statistical significance was characterized by a *P*-value below .05.

RESULTS

Demographic Information

Following conventional MRI screening, 5 participants were excluded from the study: 1 patient with SSNHL was found to have a small acoustic neuroma, and 4 participants had multiple cerebral infarcts. The final demographic characteristics of the remaining participants are summarized in Table 1. No significant differences were observed in age or sex among the 3 groups (all $P > .05$).

Whole-Brain Voxel-Wise Tract-Based Spatial Statistic Analysis

Comparison of Diffusion Tensor Imaging Parameters Between Sudden Sensorineural Hearing Loss and Healthy Control Groups

Compared with the HC group, the left idiopathic SSNHL group exhibited a significant increase in MD values in 3 WM clusters. These clusters included the body of the corpus callosum, bilateral internal capsules, superior corona radiata, and the left external capsule. However, no significant differences were found in FA, RD, or AD values between the left idiopathic SSNHL and HC groups (Figure 1, Table 2).

Comparison of Diffusion Tensor Imaging Parameters Between Sensorineural Hearing Loss and Healthy Control Groups

The TBSS analysis revealed significant differences in multiple WM clusters between the SNHL and HC groups. Overall, the SNHL group demonstrated significantly increased MD and RD values compared with the HC group, while FA values were significantly lower ($P < .05$). The MD values were notably elevated across multiple brain regions in

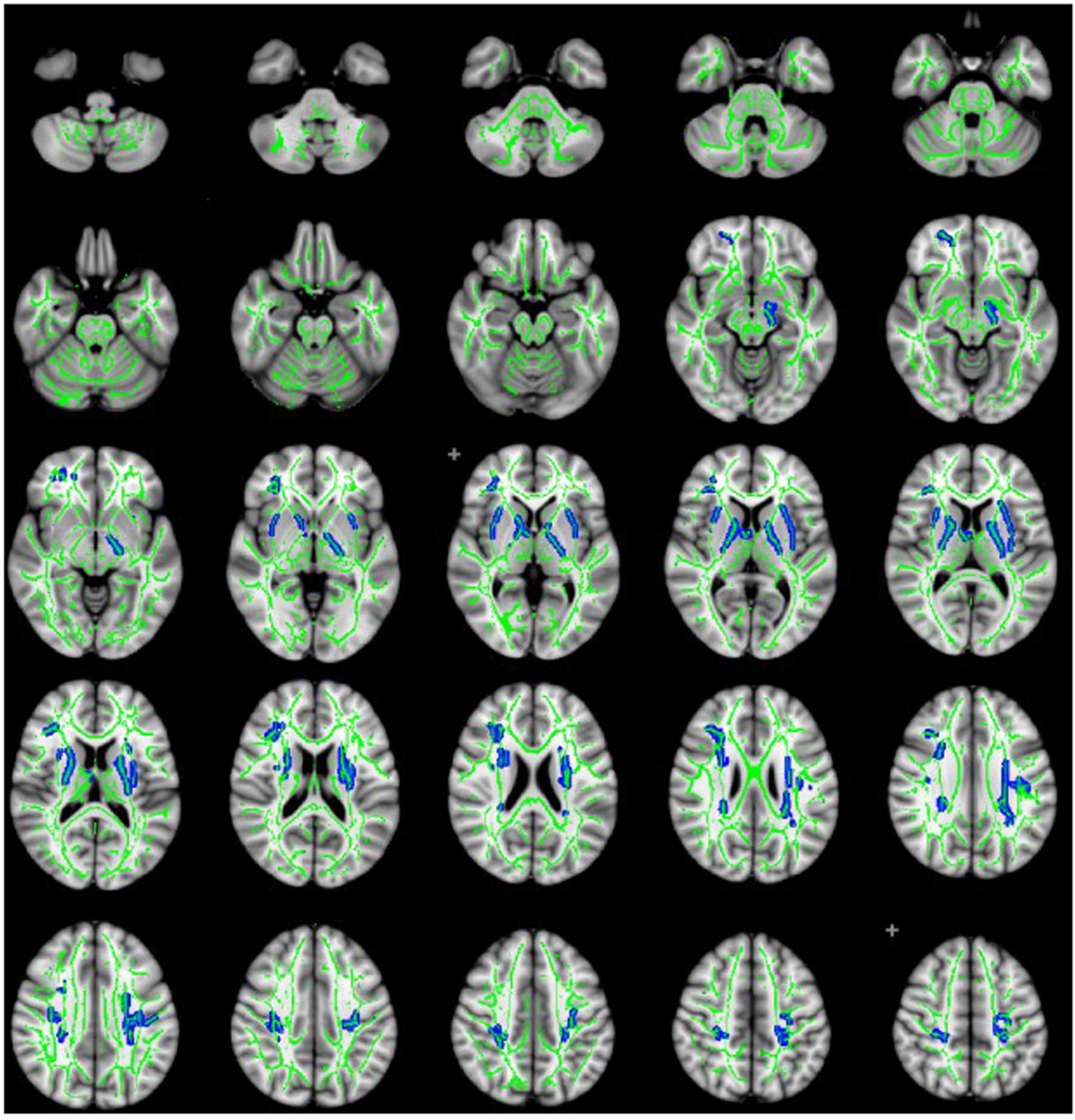

Figure 2. Whole-brain group comparison of fractional anisotropy values obtained through tract-based spatial statistics analysis ($P < .05$) between the sensorineural hearing loss and healthy control groups.

the left SNHL group, particularly in the body of the corpus callosum, left external capsule, bilateral internal capsules, and corona radiata. The regions exhibiting decreased FA values included the bilateral internal capsules, superior corona radiata, and left external capsule. Additionally, multiple regions displayed increased RD values in the SNHL group, including the body of the corpus callosum, bilateral superior corona radiata, and the left external capsule. No significant differences in AD values were detected between the two groups (Figure 2, Table 3).

Correlation Between Diffusion Tensor Imaging Parameters and Disease Duration, Interaural Latency Difference, and Auditory Brainstem Response Threshold in the SHNL Group

Compared with the HC group, 5 WM clusters exhibited significant differences in the left SNHL group. Correlation analysis was performed to assess the relationships between DTI parameter values extracted from these clusters and clinical variables, including disease duration, ILD, and ABR threshold. The results indicated that FA values in clusters 1 and 2 were negatively correlated with ABR

Table 3. Summary of Diffusion Tensor Imaging Parameters Showing Significant Differences Between the Sensorineural Hearing Loss Group and the Healthy Control Group

	Cluster Index	Voxel Size in Total	*P*	Peak MNI			Atlases (JHU ICBM-DTI-81)	Ratio of Voxels
				X	Y	Z		
FA	1	1802	.021	110	116	79	Posterior corona radiata L	28.5
				120	108	103	Superior corona radiata L	26.7
				122	128	78	External capsule L	23.6
				103	131	97	Anterior limb of internal capsule L	13.5
	2	1737	.047	62	134	101	Anterior limb of internal capsule R	40.1
				80	131	72	Posterior limbs of the internal capsules R	25.4
				69	119	81	Superior corona radiata R	18.6
MD	1	6729	.009	90	106	97	Body of corpus callosum	40.2
				117	116	93	Superior corona radiata L	22.3
				131	104	104	Superior longitudinal fasciculus L	17.3
				112	131	90	Anterior limb of internal capsule L	5.9
				121	121	82	External capsule L	5.8
				111	121	86	Posterior limbs of the internal capsules L	5.7
				115	92	98	Posterior corona radiata L	5.3
	2	4386	.009	64	115	98	Superior corona radiata R	47.2
				56	115	108	Superior longitudinal fasciculus R	24.8
				69	128	88	Anterior limb of internal capsule R	18.4
				68	120	85	Posterior limbs of the internal capsules R	11.4
RD	1	4383	.024	117	118	100	Superior corona radiata L	26.9
				90	122	98	Body of corpus callosum	23.4
				125	109	106	Superior longitudinal fasciculus L	19.7
				109	131	86	Anterior limb of internal capsule L	6.9
				123	121	80	External capsule L	5.9
				110	122	85	Posterior limbs of the internal capsules L	5.4
				16	94	101	Posterior corona radiata L	5.1
				71	119	112	Superior corona radiata R	2.5

Compared with the healthy control group, the mean diffusivity and radial diffusivity values increased and the fraction anisotropy value decreased in the sensorineural hearing loss group; Height threshold $P = .05$.

AD, axial diffusivity; DTI, diffusion tensor imaging; FA, fraction anisotropy; JHU, Johns Hopkins University; MD, mean diffusivity; MNI, Montreal neurological institute; RD, radial diffusivity.

threshold in the SNHL group. There were no significant correlations between the other clusters and the examined clinical variables (Figures 3 and 4, Table 4).

DISCUSSION

This study delineated substantial disruptions in WM microstructural integrity among cases with SSNHL and SNHL, as revealed by whole-brain voxel-wise analyses employing TBSS. The most salient findings involved escalated MD values in the corpus callosum and projection fibers in the SSNHL group, whereas the SNHL group exhibited remarkable reductions in FA alongside elevated RD in overlapping regions. These diffusion abnormalities indicate a temporospatial trajectory of WM degeneration.

Widespread microstructural anomalies were identified across several WM subsystems, involving association, projection, and commissural fibers, implicating a distributed network-level susceptibility to auditory pathology.[13-15] Notably, the corpus callosum, particularly its mid-body segment, demonstrated notably escalated MD values in SSNHL cases, a pattern suggestive of early-stage neuroinflammatory responses or extracellular fluid accumulation in the absence of overt demyelination. In contrast, SNHL cases presented with diminished FA and concomitant increases in RD in the same region, an imaging phenotype classically interpreted as indicative of progressive myelin sheath degradation with relatively intact axonal architecture. These findings are consonant with prior neuroimaging reports documenting corpus callosum degeneration in cases with long-standing SNHL, confirming the hypothesis of gradual WM compromise as a function of disease duration.

Projection fibers, which facilitate corticosubcortical and thalamocortical communication, also exhibited remarkable microstructural vulnerability. Specifically, SSNHL cases displayed escalated MD values in the bilateral corona radiata, anterior and posterior limbs of the internal capsule, and the external capsule, potentially reflecting early extracellular alterations or glial activation. In the SNHL group,

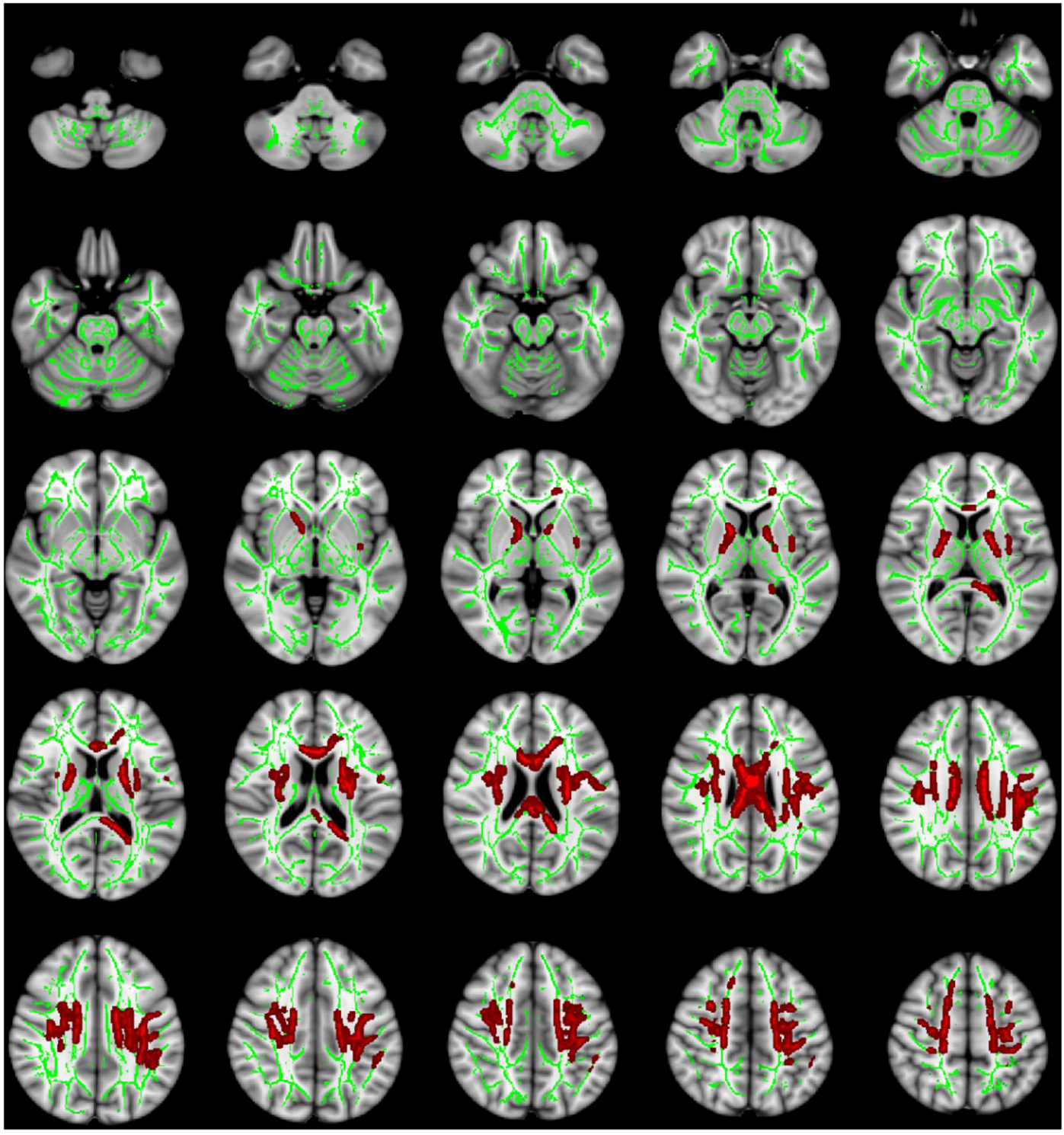

Figure 3. Whole-brain group comparison of mean diffusivity values obtained through tract-based spatial statistics analysis ($P < .05$) between the sensorineural hearing loss and healthy control groups.

however, the presence of diminished FA and escalated RD in these same regions indicated more advanced disruption of WM architecture, consistent with ongoing demyelination processes. These findings corroborate previous studies reporting altered FA within auditory radiation and associated projection pathways in both congenital and acquired forms of SNHL.[16–19]

Alterations in long-range association fibers were also noteworthy, further highlighting the widespread impact of auditory impairment on cerebral WM. Consistent with the findings of Husain et al[20] and Kim et al,[21] this investigation identified microstructural perturbations in the superior longitudinal fasciculus (SLF), inferior longitudinal fasciculus, and superior fronto-occipital fasciculus. The SSNHL group

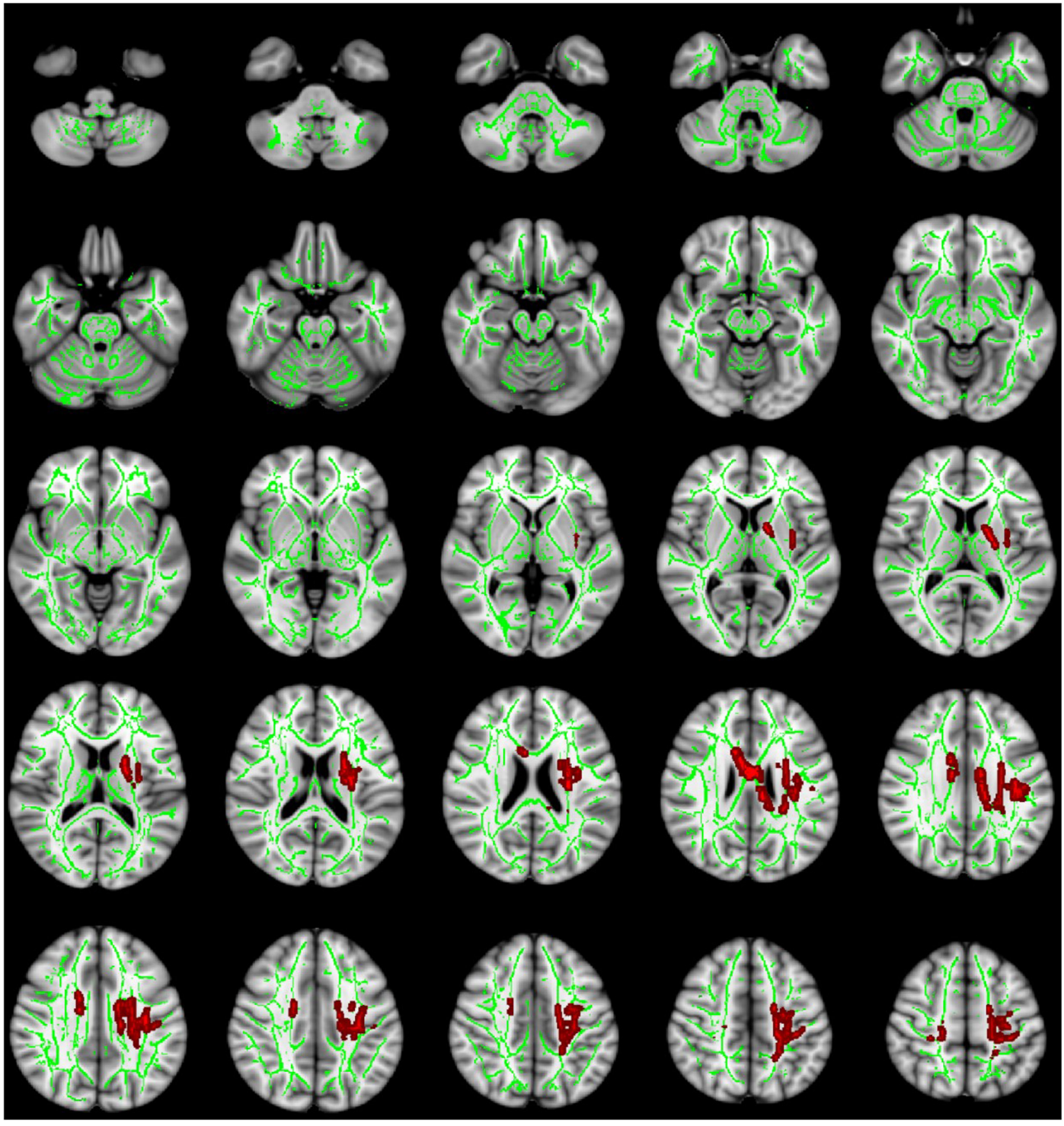

Figure 4. Whole-brain group comparison of radial diffusivity values obtained through tract-based spatial statistics analysis ($P < .05$) between the sensorineural hearing loss and healthy control groups.

demonstrated escalated MD values in the SLF, whereas the SNHL group exhibited increases in both MD and RD, with no remarkable alterations in FA. This profile may represent an early or intermediate stage of WM alteration wherein the microstructural coherence of fiber tracts is compromised without complete loss of anisotropic diffusion. The absence of FA reduction may reflect partial structural preservation, supporting theories of neuroplastic adaptation or compensatory remodeling in response to auditory deprivation.[22–25]

Furthermore, correlation analyses unveiled a notable inverse link of FA values in specific WM clusters and ABR thresholds, particularly in the SNHL group, suggesting that declining WM integrity is linked to

Table 4. Correlation Between Diffusion Tensor Imaging Parameters and the Disease Duration, Interaural Latency Difference, and Auditory Brainstem Response Threshold in the SHNL Group

	FA		MD		RD
	Cluster1	Cluster2	Cluster1	Cluster2	Cluster1
Duration	0.100	0.128	−0.016	−0.175	−0.125
ABR threshold	−0.508*	−0.598**	0.122	0.152	0.172
V-ILD	0.175	0.264	−0.311	−0.172	−0.191

ABR, auditory brainstem response; FA, fraction anisotropy; ILD, interaural latency difference; MD, mean diffusivity; RD, radial diffusivity.
*Height threshold $P = .05$.
**Height threshold $P = .01$.

worsening auditory function. Additionally, FA values' positive correlation with ILDs is noteworthy, indicating that preserved microstructural integrity may enhance neural synchrony or conduction velocity along auditory pathways. Although the direct link of ABR indices with DTI parameters has never been extensively characterized, analogous investigations[26] have documented a positive link of FA with auditory performance outcomes in hearing-impaired populations. Moreover, Zheng et al[27] reported that an ILD threshold of ≥0.4 ms may hold diagnostic utility in distinguishing hearing impairment due to neonatal hyperbilirubinemia.

Departing from the scope of prior investigations that have predominantly concentrated on chronic SNHL, the present investigation strategically incorporated both treatment-naïve, first-episode SSNHL patients and cases with long-term SNHL, thereby enabling a cross-sectional yet temporally stratified interrogation of WM microstructural alterations. The involvement of chronic SNHL cases with auditory deprivation persisting beyond 2 years provides a quasi-longitudinal approach to delineate the spatiotemporal evolution of WM architecture in response to persistent auditory input loss. Notably, this investigation is among the first to utilize whole-brain voxel-wise TBSS as a primary analytical framework to systematically quantify WM integrity alterations in both SSNHL and chronic SNHL cohorts. By circumventing the spatial constraints and hypothesis-driven limitations inherent in traditional ROI analyses, this approach facilitates an anatomically comprehensive and data-driven elucidation of WM microstructural compromise, thereby enhancing diagnostic specificity and reducing investigator bias.

A principal novel finding of this investigation is the identification of significantly elevated MD values in the corpus callosum and corticofugal projection fibers in SSNHL cases, reflecting early-stage neuroinflammatory processes, vasogenic edema, or perturbations in the extracellular matrix prior to the onset of demyelination. This is in contrast to the well-documented reduction in FA in chronic SNHL populations documented in advance. The detection of these potentially transient diffusion abnormalities in SSNHL highlights the dynamic nature of early WM remodeling and suggests a potential for neuroprotective interventions before irreversible structural degradation ensues.

Moreover, this investigation described a previously unreported association between FA values in spatially defined WM clusters and ABR thresholds in the SNHL cohort. While prior investigations have identified FA diminution in auditory-related tracts, the outcomes implicate FA as a surrogate neuroimaging correlate of auditory neural conduction efficacy. This association not only substantiates the pathophysiological relevance of DTI metrics in auditory processing disorders but also posits FA as a candidate biomarker for quantifying disease severity and tracking neurofunctional decline.

Despite the robustness of the outcomes, certain methodological constraints merit consideration. The modest sample size limited the statistical power for subgroup analysis, precluding stratification of SNHL patients by etiology, audiometric configuration, or duration of hearing loss. Furthermore, diagnostic fluidity was noteworthy, as some patients initially categorized in the SSNHL cohort transitioned to chronic SNHL status upon longitudinal follow-up exceeding 2 years. Future investigations will benefit from longitudinal, multimodal neuroimaging designs incorporating larger, phenotypically diverse cohorts, enabling more precise mapping of the temporal trajectory of WM degeneration and elucidating mechanisms among auditory deprivation, central neuroplasticity, and cognitive-behavioral outcomes.

CONCLUSION

In conclusion, the present investigation elucidated novel patterns of early-stage and progressive alterations in WM microarchitecture associated with both SSNHL and chronic SNHL. The outcomes unveiled that auditory deprivation may precipitate microstructural disruptions across diverse WM systems, involving commissural, projection, and association fiber pathways, with evidence suggestive of progressive demyelination as the duration of hearing impairment extends. These outcomes highlight the broader neuroplastic and degenerative consequences of auditory dysfunction on cerebral WM integrity. To more comprehensively delineate the temporal trajectory and underlying neurobiological substrates of these changes, future research incorporating larger cohorts and longitudinal imaging designs is warranted.

Data Availability Statement: The dataset generated and analysed during the current study is available from the corresponding author on reasonable request.

Ethics Committee Approval: Ethical committee approval was received from the Ethics Committee of University of Jining No.1 People's Hospital (approval no.:2021-IIT-082, date: June 1, 2021) .

Informed Consent: Written informed consent was obtained from the patients/patient who agreed to take part in the study.

Peer-review: Externally peer-reviewed.

Author Contributions: Concept – R.M.; Design – R.M.; Supervision – R.M.; Resources – R.M.; Materials – L.Z., S.L., F. C.; Data Collection and/or Processing – Y.W., M.W.; Analysis and/or Interpretation – L.Z., S. L.; Literature Search – L.Z., S. L.; Writing Manuscript – L.Z., S. L.; Critical Review – F.C.

Declaration of Interests: The authors have no conflicts of interest to declare.

Funding: The authors declare that this study received no financial support.

REFERENCES

1. Michel O, Deutsche Gesellschaft für Hals-Nasen-Ohren-Heilkunde, Kopf- und Hals-Chirurgie. The revised version of the german guidelines

"sudden idiopathic sensorineural hearing loss". *Laryngorhinootologie*. 2011;90(5):290-293. [CrossRef]
2. Chandrasekhar SS, Tsai Do BS, Schwartz SR, et al. Clinical practice guideline: sudden hearing loss (update). *Otolaryngol Head Neck Surg*. 2019;161(1_suppl):S1-S45. [CrossRef]
3. Ha YR, Kim D, Kim SS, Lee JM, Kim SH, Yeo SG. Comparison of recovery rates of sudden sensorineural hearing loss by age group. *J Clin Med*. 2024;13(16):4937. [CrossRef]
4. Perez Ferreira Neto A, da Costa Monsanto R, Dore Saint Jean L, et al. Clinical profile of patients with unilateral sudden sensorineural hearing loss: correlation with hearing prognosis. *Otolaryngol Head Neck Surg*. 2021;165(4):563-570. [CrossRef]
5. Tarabichi O, Kozin ED, Kanumuri VV, et al. Diffusion tensor imaging of central auditory pathways in patients with sensorineural hearing loss: a systematic review. *Otolaryngol Head Neck Surg*. 2018;158(3):432-442. [CrossRef]
6. Steele CJ, Bailey JA, Zatorre RJ, Penhune VB. Early musical training and white-matter plasticity in the corpus callosum: evidence for a sensitive period. *J Neurosci*. 2013;33(3):1282-1290. [CrossRef]
7. Karns CM, Stevens C, Dow MW, Schorr EM, Neville HJ. Atypical white-matter microstructure in congenitally deaf adults: A region of interest and tractography study using diffusion-tensor imaging. *Hear Res*. 2017;343:72-82. [CrossRef].
8. Rachakonda T, Shimony JS, Coalson RS, Lieu JEC. Diffusion tensor imaging in children with unilateral hearing loss: a pilot study. *Front Syst Neurosci*. 2014;8:87. [CrossRef]
9. Huang L, Zheng W, Wu C, et al. Diffusion tensor imaging of the auditory neural pathway for clinical outcome of cochlear implantation in pediatric congenital sensorineural hearing loss patients. *PLoS One*. 2015;10(10):e0140643. [CrossRef]
10. Wang S, Chen B, Yu Y, et al. Alterations of structural and functional connectivity in profound sensorineural hearing loss infants within an early sensitive period: a combined DTI and fMRI study [published correction appears in Dev]. *Cogn Neurosci*. 2020;41:100689.
11. Qi R, Su L, Zou L, Yang J, Zheng S. Altered gray matter volume and white matter integrity in sensorineural hearing loss patients: a VBM and TBSS study. *Otol Neurotol*. 2019;40(6):e569-e574. [CrossRef]
12. Jiang M, Wen Z, Long L, et al. Assessing cerebral white matter microstructure in children with congenital sensorineural hearing loss: A tract-based spatial statistics study. *Front Neurosci*. 2019;13:597. [CrossRef]
13. Mahmoud W, Elshawaf W, Tawfik A. The role of diffusion tensor imaging in idiopathic sensorineural hearing loss: is it significant? *Pol J Radiol*. 2021;86:e474-e480. [CrossRef]
14. Wu CM, Ng SH, Wang JJ, Liu TC. Diffusion tensor imaging of the subcortical auditory tract in subjects with congenital cochlear nerve deficiency. *AJNR Am J Neuroradiol*. 2009;30(9):1773-1777. [CrossRef]
15. Chang Y, Lee HR, Paik JS, Lee KY, Lee SH. Voxel-wise analysis of diffusion tensor imaging for clinical outcome of cochlear implantation: retrospective study. *Clin Exp Otorhinolaryngol*. 2012;5(suppl 1):S37-S42. [CrossRef]
16. Li Y, Ding G, Booth JR, et al. Sensitive period for white-matter connectivity of superior temporal cortex in deaf people. *Hum Brain Mapp*. 2012;33(2):349-359. [CrossRef]
17. Lin Y, Wang J, Wu C, Wai Y, Yu J, Ng S. Diffusion tensor imaging of the auditory pathway in sensorineural hearing loss: changes in radial diffusivity and diffusion anisotropy. *J Magn Reson Imaging*. 2008;28(3):598-603. [CrossRef]
18. Luan Y, Wang C, Jiao Y, Tang T, Zhang J, Teng GJ. Dysconnectivity of multiple resting-state networks associated with higher-order functions in sensorineural hearing loss. *Front Neurosci*. 2019;13:55. [CrossRef]
19. Miao W, Li J, Tang M, et al. Altered white matter integrity in adolescents with prelingual deafness: a high-resolution tract-based spatial statistics imaging study. *AJNR Am J Neuroradiol*. 2013;34(6):1264-1270. [CrossRef]
20. Husain FT, Medina RE, Davis CW, et al. Neuroanatomical changes due to hearing loss and chronic tinnitus: a combined VBM and DTI study. *Brain Res*. 2011;1369:74-88. [CrossRef]
21. Kim DJ, Park SY, Kim J, Lee DH, Park HJ. Alterations of white matter diffusion anisotropy in early deafness. *NeuroReport*. 2009;20(11):1032-1036. [CrossRef]
22. Ackermann C, Andronikou S, Saleh MG, et al. Early antiretroviral therapy in HIV-infected children is associated with diffuse white matter structural abnormality and corpus callosum sparing. *AJNR Am J Neuroradiol*. 2016 December;37(12):2363-2369. [CrossRef]
23. Yeh FC, Wedeen VJ, Tseng WYI. Generalized q-sampling imaging. *IEEE Trans Med Imaging*. 2010;29(9):1626-1635. [CrossRef]
24. Shaikh S, Kumar A, Bansal A. Diffusion tensor imaging: an overview. *Neurol India*. 2018;66(6):1603-1611. [CrossRef]
25. Eggermont JJ. Auditory brainstem response. *Handb Clin Neurol*. 2019;160:451-464. [CrossRef]
26. Krumbholz K, Hardy AJ, de Boer J. Automated extraction of auditory brainstem response latencies and amplitudes by means of non-linear curve registration. *Comput Methods Programs Biomed*. 2020;196:105595. [CrossRef]
27. Zheng Z, Liu HY, Yang SP, Du LZ. Association between the inter-aural latency difference of brainstem auditory evoked potential wave V and neonatal hyperbilirubinemia. *Zhongguo Dang Dai Er Ke Za Zhi*. 2021;23(5):499-504. [CrossRef]